The Astrophysical Journal Letters, 906:L4 (6pp), 2021 January 1 https://doi.org/10.3847/2041-8213/abcecb

Physics of Nonuniversal Larson's Relation

Renyue Cen
Princeton University Observatory, Princeton, NJ 08544, USA; cen@astro.princeton.edu
Received 2020 June 29; revised 2020 November 23; accepted 2020 November 24; published 2021 January 6

Abstract

From a new perspective, we reexamine self-gravity and turbulence jointly, in hopes of understanding the physical basis for one of the most important empirical relations governing clouds in the interstellar medium (ISM), the Larson's relation relating velocity dispersion (σ_R) to cloud size (R). We report on two key new findings. First, the correct form of the Larson's relation is $\sigma_R = \alpha_v^{1/5}\sigma_{\rm pc}(R/1\ {\rm pc})^{3/5}$, where α_v is the virial parameter of clouds and $\sigma_{\rm pc}$ is the strength of the turbulence, if the turbulence has the Kolmogorov spectrum. Second, the amplitude of Larson's relation, $\sigma_{\rm pc}$, is not universal, differing by a factor of about 2 between clouds on the Galactic disk and those at the Galactic center, as evidenced by observational data.

Unified Astronomy Thesaurus concepts: Interstellar medium (847); Diffuse interstellar clouds (380); Gravitational interaction (669); Interstellar clouds (834); Interstellar dynamics (839); Gravitational equilibrium (666); Gravitational collapse (662); Star formation (1569); Interstellar magnetic fields (845); Dark interstellar clouds (352); Dense interstellar clouds (371)

1. Introduction

The interstellar medium (ISM) in galaxies is subject to a myriad of physical processes, including gravitational interactions, inflow and outflow, radiative processes, magnetic field, and feedback from stellar evolution (e.g., McKee & Ostriker 2007) and thus, perhaps unsurprisingly, bears a chaotic and turbulent appearance (e.g., Elmegreen & Scalo 2004). The role of supersonic turbulence in interacting with the process of gravitational collapse of molecular clouds has long been recognized (e.g., Larson 1981). We inquire and seek solutions as to why ISM clouds appear to follow a number of well-defined empirical governing relations, by examining together the two most important physical processes—turbulence and self-gravity—guided by a new conceptual insight. Our goal is not set out to precisely nail down these relations, but rather to make sense of complex players involved, in a simple fashion, if possible. The results we find are gratifyingly simple and accurate.

The turbulence in the ISM is driven at some large scales. In incompressible turbulence, the structure function is derived by Kolmogorov (1941), most notably the expression for the relation between the velocity difference between two points and their separation, $\sigma_R \propto R^{1/3}$, based on a constant energy transmission rate through the inertia scale range. In highly compressible turbulence, the energy transmission down through the scale is no longer conservative, with kinetic energy also being spent to shock and/or compress the gas. Thus, if the relation remains a scale-free power law, the resulting exponent for a compressive turbulent medium is expected to be larger than $1/3$. We will show that the right exponent is $3/5$ in this case.

Opposite to the driving scale, the "coherence" scale in dense cores, introduced in Goodman et al. (1998), encapsulates the transition from turbulence-dominated energy regime to a subsonic regime, where the sum of the thermal, magnetic, and possibly other forms of energy dominates over turbulent energy. The turbulence is then often thought of cascading down between these two scales. In contrast to this simple cascading (down) of eddies in the gravity-free case, a new conceptual notion that we put forth here is that the dynamic interactions between turbulence and gravity occurring on all scales result in the formation of clouds, within which self-gravitational force becomes important (not necessarily dominant in general), on all scales. While the formation of clouds is originally driven by supersonic turbulence, gravity acts to both solidify them and in some cases detach them from the turbulence, and hence provides a feedback loop to the turbulence itself, where the clouds may be visualized as the boundary conditions (on all scales) for the turbulence. As such, we shall call such an additionally constrained turbulence a "cloud bound turbulence chain" (CBTC), as opposed to a gravity-free turbulence. The singular coherence scale ($\sim$0.1 pc) above represents the smallest cloud of our CBTC. Based on this conception, we attempt to rederive the (revised) Larson's relation, and compare to observations.

2. Larson's Relation: Confluence of Supersonic Turbulence and Self-gravity

In the ISM, self-gravity has the tendency to organize and fortify suitable regions into their own entities, playing a countervailing role against supersonic turbulence that would otherwise produce only transient structures. For a power-law radial density profile of slope $-\beta$, the self-gravitating potential energy is $W = -\frac{3-\beta}{5-2\beta}\frac{GM_R^2}{R}$, where R and M are the radius and mass of the cloud. As we will show later, the density profile of gas clouds in the supersonic regime is expected to have $\beta = 4/5$; thus, we will use $W = -\frac{11}{17}\frac{GM^2}{R}$ for all subsequent calculations. For a self-gravitating sphere of the same density profile, the mean velocity dispersion within radius R is related to the 1D velocity dispersion at separation R by $\bar{\sigma}_R{}^2 = \frac{11}{14}\sigma_R^2$. However, it proves more convenient to use $\bar{\sigma}_R$ instead of σ_R, since the former is a more used observable.

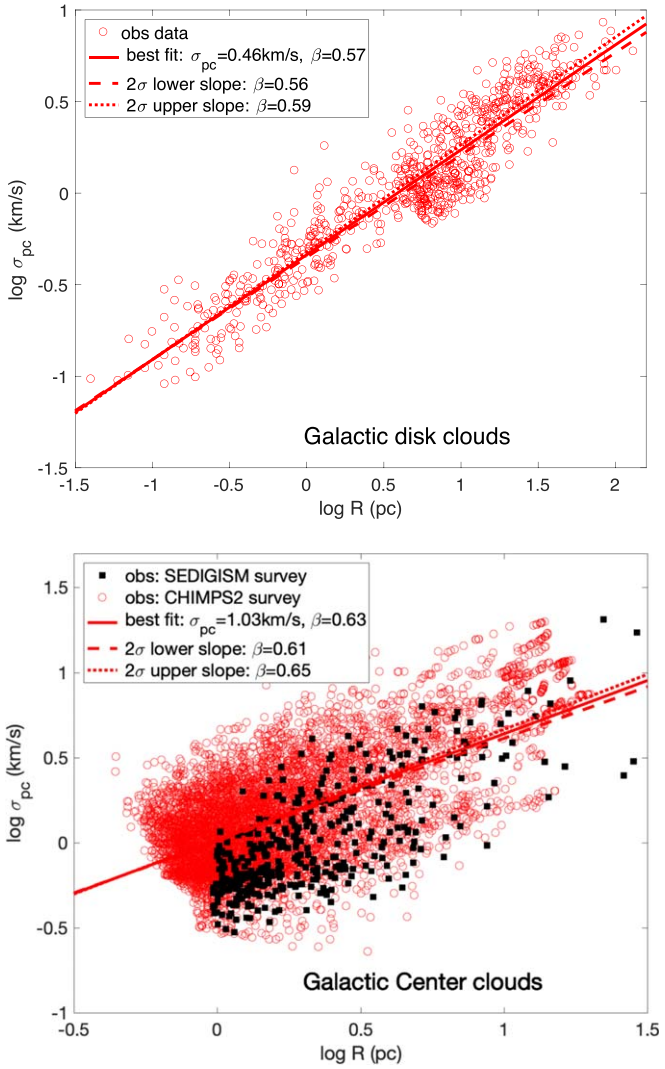

Figure 1. Top panel shows the velocity as a function of its size for the observed molecular clouds on the Galactic disk (open red circles), from Dame et al. (1986), Solomon et al. (1987), Heyer et al. (2001), Heyer & Brunt (2004), Ridge et al. (2006), Narayanan et al. (2008), and Ripple et al. (2013). Bottom panel shows the velocity as a function of its size, for the observed molecular clouds at the Galactic center from the CHIMPS2 survey (Eden et al. 2020; open red circles) and the SEDIGISM (Duarte-Cabral et al. 2021; solid black squares). In each panel, we show as red solid line as the best power-law fit using linear regression, along with the 2σ upper and lower slopes shown as dotted and dashed lines, respectively, obtained with bootstrapping.

Hence, we shall use $\bar{\sigma}_R$ for all subsequent expressions; for brevity, we use σ_R to represent $\bar{\sigma}_R$ hereafter. To reduce cumbersomeness in expressions, we neglect all other forms of energy but only to keep the gravitational energy W and gas kinetic energy K; it is straightforward to include those neglected, by modifying the expression for virial parameter. We thus define the virial parameter α_v as $\alpha_v = -\frac{2K}{W}$.

The self-gravitating tendency may then be formulated as a 3D region in the 4D parameter space of (R, σ_R, ρ_R, α_v):

$$\sigma_R^2 = \alpha_v \frac{11}{51}\frac{GM}{R} = \alpha_v \frac{44\pi}{153} G\rho_R R^2 = \alpha_v \frac{11\pi}{51} G\Sigma_R R, \quad (1)$$

where G is gravitational constant, and ρ_R and Σ_R are the mean volume and surface density within radius R. If α_v and σ_R are independent, which we will show is the case, the region would look like a thick plane. Equation (1) is essentially the proposed modification to Larson's relation by Heyer et al. (2009). More comparisons will be made in Section 3.

The Kolmogorov (1941) power spectrum is derived for homogeneous and isotropic 3D subsonic turbulence in incompressible flows, valid in the energy conserving inertial range. In contrast, the kinetic energy in the supersonic compressible turbulence in the ISM is dissipative on all scales due to shocks and radiative processes. It thus, at the first instant, might suggest that the Kolmogorov turbulence may provide an inadequate description of the compressible turbulence of the ISM.

Fleck (1983) suggests that the relation between a scaled velocity v_R and scale R of compressible turbulence be expressed as

$$v_R \equiv \rho_R^{1/3}\sigma_R = AR^{1/3}, \quad (2)$$

which constitutes a plane in the parameter space of (R, σ_R, ρ_R), generally different from that of self-gravity (Equation (1)), where A is a constant. The expression essentially asserts that a constant volumetric energy density transfer rate in compressible flow is transmitted down the turbulence cascading scale. Equation (2) reduces to the original Kolmogorov form for incompressible flow that is a line in the 2D parameter space of (R, u_R). A formal proof of the existence of an inertial range for highly compressible turbulence is given by Aluie (2011, 2013), validating the density-weighted velocity formulation. Importantly, numerical simulations show that the spectrum of v_R indeed follows the Kolmogorov spectrum remarkably well for the isothermal ISM (e.g., Kritsuk et al. 2007, 2013). We thus continue to use the nomenclature of Kolmogorov compressible turbulence, despite it sounding like an oxymoron, given the spectral slope we adopt and its empirical validity to describe the turbulence of the isothermal ISM. The general physical arguments and quantitative conclusions reached are not altered much with relatively small variations of the slope of the turbulence power spectrum.

On a related note, in the subsonic compressible turbulence, with gravity also playing an important role, such as in dark cores in molecular clouds, the physical premise for the argument of energy transmission through the inertia scale range ceases to apply with respect to the total velocity. This may be understood in that the turbulence chain driven at some large scales no longer is the primary driver of velocity in the subsonic regime. Rather, the velocity field is driven jointly by turbulence, thermal (and possibly other forms of) pressure, and gravity (Myers 1983).

Combining Equations (1) and (2) gives

$$\sigma_R = \alpha_v^{1/5}\left(\frac{44}{153}A^3 G\right)^{1/5} R^{3/5}. \quad (3)$$

Because A is unknown but a constant, we simply introduce another parameter, $\sigma_{\rm pc}$, which denotes the 1D mean turbulence velocity dispersion within a region of radius 1 pc, to express the strength of the turbulence. Now Equation (3) is simplified to

$$\sigma_R = \alpha_v^{1/5}\sigma_{\rm pc}\left(\frac{R}{1\ {\rm pc}}\right)^{3/5}. \quad (4)$$

Looking at Equation (4), it may seem puzzling as to why the virial parameter α_v appears in this expression that is supposedly an expression of the strength of the turbulence chain. But it is expected. The appearance of α_v (and the disappearance of gas density ρ) in this expression reflects the feedback of the boundary condition at the clouds that terminates the turbulence chain at the small scale end, in lieu of gas density. To see that we may express the cloud density in terms of $\sigma_{\rm pc}$,

$$n_{\rm pc} = \alpha_v^{-3/5}\frac{153}{44\pi}\frac{\sigma_{\rm pc}^2}{Gm_p(1\ {\rm pc})^2} = 1.04\ \times\ 10^4\ {\rm cm^{-3}}\alpha_v^{-3/5}\left(\frac{\sigma_{\rm pc}}{1\ {\rm km\ s^{-1}}}\right)^2, \quad (5)$$

where n_{pc} is the mean density within a cloud of radius 1 pc with a virial parameter α_v.

Equation (4) is the (revised) Larson's first relation, relating the velocity dispersion to the size of the cloud. Let us now proceed to compare this relation to observational data. Figure 1 shows the observational data along with best power-law fits. We fit the data to a power law of the form

$$\sigma_R = \alpha_v^{1/5}\sigma_{\rm pc}\left(\frac{R}{1\ {\rm pc}}\right)^{\beta}, \quad (6)$$

leaving both the amplitude $\sigma_{\rm pc}$ and the exponent β as two free parameters. Moreover, we perform bootstrap resampling to obtain upper and lower 2σ limits of the fitting parameters by fitting both parameters. We find the best parameters and the $\pm 2\sigma$ limits for the disk clouds to be

$$\begin{aligned} &\text{best fit:}\ \ \sigma_{\rm pc} = 0.46 \pm 0.03\ \ {\rm km\ s^{-1}} \text{and}\ \beta = 0.57 \pm 0.02\\ &+2\sigma:\quad \sigma_{\rm pc} = 0.48 \qquad\qquad \text{and}\ \beta = 0.59\\ &-2\sigma:\quad \sigma_{\rm pc} = 0.45 \qquad\qquad \text{and}\ \beta = 0.56, \end{aligned} \quad (7)$$

shown as the solid, dotted, and dashed lines, respectively, in the top panel of Figure 1. Repeating the calculation for the clouds at the Galactic center yields the best parameters and the $\pm 2\sigma$ limits:

$$\begin{aligned} &\text{best fit:}\ \ \sigma_{\rm pc} = 1.03 \pm 0.01\ \ {\rm km\ s^{-1}} \text{and}\ \beta = 0.63 \pm 0.01\\ &+2\sigma:\quad \sigma_{\rm pc} = 1.02 \qquad\qquad \text{and}\ \beta = 0.65\\ &-2\sigma:\quad \sigma_{\rm pc} = 1.05 \qquad\qquad \text{and}\ \beta = 0.61, \end{aligned} \quad (8)$$

shown as the solid, dotted, and dashed lines, respectively, in the bottom panel of Figure 1. We note that the error bars of the best fit using the linear regression method is not necessarily consistent with and often larger than the 2σ range obtained using bootstrap, due to the latter's larger sample size with bootstrapping. The discrepancy is more noticeable for the disk clouds due to the smaller observational data sample size, as compared to that of the Galactic center clouds. Nevertheless, even in the absence of this shift for the best slope, the traditional exponent of the Larson's relation of $1/2$ is inconsistent with the disk data at 100% level if the bootstrap is used and at 3.5σ if the direct regression is used, whereas a slope of 0.6 is about 1.5σ away. If considering the clouds at the Galactic center, the contrast is still larger.

So far, we have not considered possible (perhaps different) systematics for the observations of the Galactic disk clouds as compared to the Galactic center clouds. The fact that the best-fitting slope of the disk clouds of 0.57 and that of the Galactic center clouds of 0.63 equidistantly flank our proposed slope of 0.60 is intriguing. It may be caused by some additional physics that are not considered in our simplified treatment but operates to varying degrees of importance in these cases. It may also be caused by data inhomogeneities in the plotted plane, which may already be visible. We take the simpler interpretation that both slopes are intrinsically equal to 0.60 and the apparent values are due to some observational systematics, although we are not in a position to justify this assertion.

This new Larson's relation with the exponent $3/5$ is in excellent agreement with observational data. Heyer & Brunt (2004) measure the value of the scaling exponent of 0.59 ± 0.07 in the spatial range of 1–50 pc (corresponding to the original range of Larson 1981 and Solomon et al. 1987), while fitting the entire spatial range of 0.03–50 pc probed they get 0.62 ± 0.09.

It is clear now that it is not just the gravity alone that gives rise to Larson's relation, rather it is a combination of gravity and turbulence physics that naturally yields it. Larson (1981) invoked virial equilibrium to explain his relation. What is new here is that the intersection of gravity and turbulence provides a significantly better fit for data. Forcing the slope of 0.6 to both data sets, the best fit $\sigma_{\rm pc}$ is found to be

$$\begin{aligned} &\sigma_{\rm pc} = 0.44 \pm 0.02\ {\rm km\ s^{-1}}\ \text{for Galactic disk clouds}\\ &\sigma_{\rm pc} = 1.08 \pm 0.01\ {\rm km\ s^{-1}}\ \text{for Galactic center clouds.} \end{aligned} \quad (9)$$

From data in our Galaxy alone, one can thus already conclude that CBTCs vary in different environments within a galaxy. A two-sample KS test between the $\sigma_{\rm pc}$ distribution of the Galactic disk clouds and that of the Galactic center clouds gives a p-value $p = 5 \times 10^{-20}$, indicating they are statistically different. It follows then that CBTCs and hence Larson's relation may vary across galaxies and in different environments within galaxies. This prediction is supported by recent observations of molecular clouds in other galaxies (e.g., Donovan Meyer et al. 2013; Hughes et al. 2013; Colombo et al. 2014; Krieger et al. 2020).

Historically, from Equation (1) we see that, if one insists expressing Larson's first relation with the exponent close to 0.5, the original Larson's first relation would be gas cloud surface density dependent, a point later reiterated (Heyer et al. 2009). But if the range in Σ_R is sufficiently narrow, one would obtain the original scale of a slope of $1/2$, which may be the reason for that result obtained by Larson (1981). Thus, the original Larson's first relation has a limited scope and is applicable only when the range of surface density is narrow enough. In contrast, the revised Larson's relation, Equation (4), is expected to be valid universally, except that the strength parameter, $\sigma_{\rm pc}$, is expected to vary across different environments and across galaxies. To illustrate this point better, let us express $\sigma_{\rm pc}$ in terms of direct observables, involving gas surface density. Combining Equations (1) and (4) gives

$$\sigma_{\rm pc} = \alpha_v^{3/10}\left(\frac{\Sigma_R}{341\ M_\odot\ {\rm pc^{-2}}}\right)^{1/2}\left(\frac{R}{1\ {\rm pc}}\right)^{-1/10}\ {\rm km\ s^{-1}}. \quad (10)$$

The large difference between Larson's relation for the disk clouds and the Galactic center clouds strongly indicates an important role played by turbulence and that the CBTCs in the disk and at the Galactic centers are different, since gravity is the same. While one may use Equations (4) or (10) or other variants to drive $\sigma_{\rm pc}$ empirically with three observables, such a derivation does not address the physical origin of the magnitude of $\sigma_{\rm pc}$. A simple top-down illustrative method to derive $\sigma_{\rm pc}$ is given in Section 4.

We should note that our adoption of the Kolmogorov turbulence spectrum is largely motivated by available simulations. The obtained consistency with observations suggests it may be valid. The agreement with the observed fractal dimension in Section 3 is consistent with Kolmogorov spectrum as well. Nonetheless, in general, the turbulence spectrum may not adhere strictly to that of Kolmogorov type. A more general form of Equation (4) may be written as

$$\sigma_{\rm R} \propto \alpha_v^{1/5} R^{(3\phi+2)/5}. \quad (11)$$

For the Kolmogorov turbulence, we have $\phi = 1/3$, which yields an exponent of 0.6. For Burgers (1948) turbulence, we have $\phi = 1/2$, corresponding to an exponent 0.7, while the turbulence in a strong magnetic field may have an Iroshnikov–Kraichnan (Iroshnikov 1964; Kraichnan 1965) type with $\phi = 1/4$, which would yield an exponent of 0.55. If one were to ascribe the difference in the exponent for the Galactic disk and Galactic center clouds to physical differences in the respective turbulence, one way to reconcile these two different exponents is that the turbulence on the Galactic disk is closer to that of Iroshnikov–Kraichnan type than the turbulence at the Galactic center. This requires further work to clarify, which is beyond the scope of this Letter. Nonetheless, none of different types of turbulence is expected to yield the conventional exponent for the Larson's relation of 0.5.

Another point worth noting is that there are clouds with $\alpha_v < 1$, i.e., overvirialized clouds. Obviously, these clouds seem unlikely to be evolutionary descendants of clouds that had $\alpha = 1$ and subsequently endured some gravitational collapse. If that were the case, it would imply a turbulence dissipation time significantly less than the freefall time of the system, inconsistent with simulations (e.g., Stone et al. 1998). Therefore, we suspect that these low α_v systems are a direct product of turbulence, clouds that have relatively low velocity dispersion for their gravitational strength and are probably transient, due to the randomness of the turbulence.

To further clarify the nature of these special clouds, we show in Figure 2 the cloud mass as a function of its virial parameter. To our surprise, clouds with $\alpha_v < 1$ span the entire mass range. This may be consistent with the randomness of the turbulence suggested above. We note, however, that some of the most massive clouds ($\geqslant 10^6\,M_\odot$), i.e., giant molecular clouds, may be a collection of uncommunicative, smaller clouds in an apparent contiguous region, where the measured velocity dispersions reflect those of their smaller constituents, while the overall gravitational energy increases with congregation; we note that the velocity dispersion in this case may be significantly anisotropic. Finally, the ubiquitous existence of gravitationally unbound clouds is simply due to insufficient gravitational force relative to the turbulence velocity field in these clouds. A point made here is that gravitationally unbound clouds are not necessarily those that become gravitationally bound first and later become unbound due to internal stellar feedback or cloud–cloud collisions (e.g., Dobbs et al. 2011).

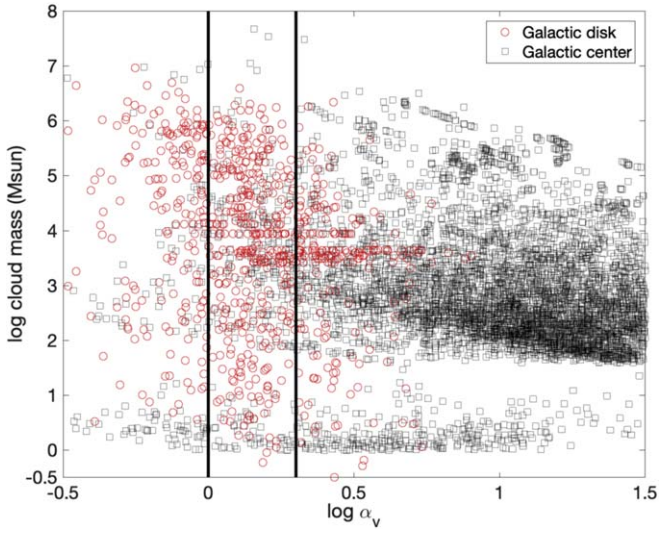

Figure 2. Cloud mass as a function of α_v for the Galactic disk clouds (open red circle) and Galactic center clouds (open black squares). The two vertical lines indicate clouds with $\alpha_v = 1$ and 2, respectively, for reference.

In Figure 2 it is seen that the clouds at the Galactic center (black squares) show a noticeable gap in mass, from $\sim 3\,M_\odot$ to $\sim 30\,M_\odot$. It is not clear to us what might have caused this. There is a separate ridge (horizontally oriented) of clouds near the bottom of the plot for the Galactic center clouds with masses around one solar mass. These low-mass clouds appear to be mostly unbound. While it is not definitive, these clouds may be the counterpart of subsolar mass clouds on the Galactic disk called "droplets" with odd "virial" properties (Chen et al. 2019a, 2019b), although we are not sure why their typical mass is about $1\,M_\odot$ instead of $\sim 0.4\,M_\odot$ found for the droplets. These small systems have large virial parameters but remain bound by external (thermal and turbulent) pressure. The connection between these systems and the CBTC that we envision here may no longer be direct, and considerations of some additional physics may be required to place these systems also within the general framework outlined here. We defer this to a later work.

Another word to further clarify the physical meaning of Equation (4) may be in order, which, let us recall, is a result derived based on the joint action of the statistical order imposed by turbulence of strength $\bar{\sigma}_{\rm pc}$ (with a small dispersion) and the natural selection effect by self-gravity, with (the inverse of) α_v describing the strength of the latter acting against the former. If α_v is much greater than unity, gravitational force would be too feeble to hold the cloud together long enough to dissipate the excess energy to allow for further consistent gravitational contraction in the presence of internal and external disruptive force of turbulence. Thus, the observed clouds with α_v greatly exceeding unity that are products of supersonic turbulence are likely transient in nature. Nonetheless, they may be useful for some physical analysis. They may be considered good candidates for analyses where a statistical equilibrium is a useful assumption. At the other end, when α_v is close to unity, gravitational collapse of a cloud may ensue, detaching it from the parent CBTC. However, as noted in Figure 2, one should exercise caution to treat clouds with an apparent α_v less than unity that may not be genuinely coherent gravitational entities, ready to run away and collapse. We shall not delve into this further but note that these apparently overvirialized clouds may

not possess the usual gravitationally induced density stratification and may lack a coherent structure (such as a well-defined center).

3. Fractal Dimension of the ISM

Using Equations (1) and (4), we may express the cloud density–size relation:

$$n_R = \alpha_v^{-3/5}\frac{153}{44\pi}\frac{\sigma_{\rm pc}^2}{Gm_p(1\ {\rm pc})^2}\left(\frac{R}{1\ {\rm pc}}\right)^{-4/5}$$
$$= 1.0\times 10^4\alpha_v^{-3/5}\left(\frac{\sigma_{\rm pc}}{1\ {\rm km\ s^{-1}}}\right)^2\left(\frac{R}{1\ {\rm pc}}\right)^{-4/5}\ {\rm cm^{-3}}, \quad (12)$$

where n_R is the mean hydrogen number density within radius R and m_p is proton mass. Then, the size–cloud mass relation follows

$$M_R = 2.6\times 10^2\alpha_v^{-3/5}\left(\frac{\sigma_{\rm pc}}{1\ {\rm km\ s^{-1}}}\right)^2\left(\frac{R}{1\ {\rm pc}}\right)^{11/5} M_\odot. \quad (13)$$

Since α_v and R are uncorrelated, for clouds generated by the same CBTC (a $\sigma_{\rm pc}$ with dispersion), we see that $M_R \propto R^{11/5}$. This mass–size relation with a slope of 2.2 is in excellent agreement with the observed values of 2.2 ± 0.1 (Heyer et al. 2001) and 2.36 ± 0.04 (Roman-Duval et al. 2010).

There are many different techniques used to measure cloud mass and size. We stress that the size–mass relation depends on how clouds are defined or selected. For the same reason that the original Larson's size–velocity dispersion relation has an exponent of $1/2$, the original Larson's size–mass relation has an exponent of 2. Both are due to a small surface density range of the clouds (e.g., Beaumont et al. 2012). The exponent in Equation (13) expresses the size–mass relation for clouds at a fixed virial parameter.

In the context of a fractal, self-similar structure, which may approximate the ISM reasonably well, Equation (13) indicates that the fractal dimension of the ISM is $D = 2.2$ (Mandelbrot 1983) with the implied size function of the form

$$n(L)dL \propto L^{-D-1}dL \propto L^{-16/5}dL. \quad (14)$$

The slope $16/5$ in Equation (14) is in excellent agreement with the observed value of 3.2 ± 0.1 for CO-detected molecular clouds in the Milky Way spanning the range of $\sim$1–100 pc (Heyer et al. 2001).

The fractal dimension of the ISM of $D = 2.2$ corresponds to density power spectrum of $P_k \propto k^{D-3} \propto k^{-0.8}$. It is helpful to have an intuitive visualization of this outcome. In the process of energy transmitting downward along the spatial/mass scale via supersonic motion, shocks, and radiative cooling, the density structure (density fluctuation spectrum) is generated. In three-dimensional space, an ideal, long and uniform filament will have a density power spectrum $P_k \propto k^{-1}$ on scales below the length of the filament. Similarly, a uniform sheet corresponds to $P_k \propto k^{-2}$, whereas a point corresponding to a density power spectrum of $P_k = k^0$. In the absence of self-gravity, compressive supersonic turbulence with sufficient cooling has the tendency to form filaments where two planar shocks intersect. In realistic situations with self-gravity, filaments have varying lengths and the actual density power spectrum is expected to deviate somewhat from this, depending on the nature of driving and energy distribution of the driving, and the power spectrum is in general $P_k \propto k^{-\beta}$ with $\beta < 1$. Nevertheless, as long as the energy in the turbulence is dominated on the large scales, β is not likely to be much less than unity. Thus, we see that the Kolmogorov compressive turbulence generated, gravitationally significant structures, in the presence of rapid radiative cooling, have a density structure that is dominated by filamentary structures with a small mixture of knots.

4. Estimate $\sigma_{\rm pc}$ for Viscously Driven Turbulence

In the normal situation where star formation occurs on a disk, it is reasonable to assume that the radius of the largest turbulence "cloud," which will be the driving scale of the CBTC, is equal to the scale height of the disk for isotropic turbulence. This driving scale, R_d, can be expressed as

$$R_d = \frac{CR_g\sigma_d^2(R_g)}{v_c^2(R_g)}, \quad (15)$$

where $\sigma_d(R_g)$ is the velocity dispersion on the driving scale R_d at a galactocentric radius R_g, which is also the vertical dispersion, $v_c(R_g)$ is the circular velocity at radius R_g, and C is a constant of order unity to absorb uncertainty. We assume that the energy source is the rotational energy at the location, where the turbulence may be driven by some viscous processes on the disk. With such an assertion, one can relate σ_d to R_d by

$$\sigma_d = 2BR_d\Omega(R_g), \quad (16)$$

where $\Omega(R_g)$ is the angular velocity at the radius R_g for a Mestel disk that we will adopt as a reasonable approximation, and B is another constant of order unity to absorb uncertainty. For a gas cloud (assumed to be uniform) of radius R_d, we can express the virial parameter by

$$\alpha_d = \frac{3\sigma_d^2(R_g)}{\frac{3}{5}\frac{GM_d}{R_d}} = \frac{15\sigma_d^2}{4\pi G\rho_d R_d^2}, \quad (17)$$

where ρ_d is the gas density at the driving scale. With Equations (15)–(17) we can compute $\sigma_{\rm pc}$ using Equation (4):

$$\sigma_{\rm pc} = 0.44\ {\rm km\ s^{-1}}\left(\frac{D}{2.3}\right)^{-1/5}\left(\frac{\Sigma_d}{5\ M_\odot\ {\rm pc^{-2}}}\right)^{1/5}$$
$$\times\left(\frac{v_c}{220\ {\rm km\ s^{-1}}}\right)^{3/5}\left(\frac{R_g}{8{\rm kpc}}\right)^{-2/5}, \quad (18)$$

where we have defined another constant $D \equiv B/C$. Equation (18) is expressed such that if the fiducial values are taken, we obtain $\sigma_{\rm pc} = 0.44\ {\rm km\ s^{-1}}$ for disk clouds center near the solar radius, as derived earlier (see Equation (9)). Aside from the unknown combination of D, all other fiducial values are well observed, including the gas surface density of $5\ M_\odot\ {\rm pc^{-2}}$ (e.g., Sofue 2017). Interestingly, if we use the same $D = 2.9$ value along with the relevant values for other parameters for the Galactic center, $\Sigma_d = 30\ M_\odot\ {\rm pc^{-2}}$ (Sofue 2017), $R_g = 500$ pc (within which the Galactic center clouds are observed), $v_c = 250\ {\rm km\ s^{-1}}$ (Sofue 2017), we obtain $\sigma_{\rm pc} = 2.1\ {\rm km\ s^{-1}}$, larger than the value of $1.08\ {\rm km\ s^{-1}}\pm0.01$ dex, derived for the clouds at the Galactic center (see Equation (9)). Although the expectation that $\sigma_{\rm pc}$ at

the Galactic center is larger than that on the Galactic disk is in agreement with the derived values, the numerical discrepancy may be due to a number of causes. It may be in part due to different observational systematics for disk clouds and center clouds. It may be in part due to that the treatment of the central region of the Galaxy as a disk breaks down or that the effective viscosity in the two regions is different. It is notable that our simple calculations do not require participation of some other physical processes that might be relevant, including magnetic field and stellar feedback. While this is not vigorous proof of the veracity of our assumptions, the agreement found between the predicted $\sigma_{\rm pc}$ and the directly calculated value for the Galactic center clouds is a validation of our basic assumptions and the resulting outcomes, that is, turbulence and gravity play a dominant role in shaping the ISM and the formation of clouds down to at least the sonic scale.

5. Conclusions

An analysis of a joint action of compressive turbulence and self-gravity is performed. Physically, it may be considered that the turbulence is bookended by the gravitationally significant clouds at the small scales, as opposed to the driving scale on a large scale. We denote such a turbulence chain as a "cloud bound turbulence chain" (CBTC).

The (new) Larson's relation, $\sigma_R = \alpha_v^{1/5}\sigma_{\rm pc}(R/1{\rm pc})^{3/5}$, relating the velocity dispersion σ_R to the size R of a cloud, is derived, where α_v is the virial parameter of the cloud and $\sigma_{\rm pc}$, the velocity dispersion of the turbulence at 1 pc, encodes the strength of the CBTC. Although implicit in the assumption is that the turbulence is supersonic, the new Larson's relation is shown to hold at least down to the transonic scale of 0.05 pc. The conventional exponent of $1/2$ for the Larson's relation is shown to be excluded.

The most significant finding is not necessarily the derivation of this relation naturally and the exponent $3/5$ being in good agreement with observations. It is prudent to remind ourselves that this exponent depends on the assumed Kolmogorov spectral index for the turbulence and error treatments of cloud measurements can certainly be improved, changes to either of which may change its value to some extent. Rather, the fact is, which is made plain by the analysis as well as the empirical evidence, that, while the exponent of the Larson's relation may be universal or close to universal, the amplitude, $\sigma_{\rm pc}$, is not and may differ greatly. The latter is environment dependent, reflecting the dependence of $\sigma_{\rm pc}$ of a CBTC on environment. The recognition of and evidence for the nonuniversality of the Larson's relation is of fundamental physical importance. The implications may be profound for the star formation process, which is thought to be dependent on the Mach number of turbulence, which in turn is linearly proportional to $\sigma_{\rm pc}$.

Our analysis also yields a byproduct with respect to some properties of the fractal nature of the ISM. We show that the fractal dimension of the ISM is $11/5$ and has a cloud (linear) size function of $n(R)dR \propto R^{16/5}dR$, both in nearly exact agreement with observations.

I would like to thank the referee Dr. Alyssa Goodman for a constructive report that helped significantly improve the Letter. I thank Dr. Mark Heyer for kindly providing the observational data in suitable formats, Dr. Eric Koch for kindly sharing the CHIMPS2 survey data, along with Drs. Erik Rosolowsky, David Eden, and Nico Krieger, Dr. Frederic Schuller for kindly sharing the SEDIGISM survey data, Dr. Nico Krieger for his kind help with obtaining data, and many colleagues for useful discussions. This work is supported in part by grant NASA NNX11AI23G.

ORCID iDs

Renyue Cen https://orcid.org/0000-0001-8531-9536

References

Aluie, H. 2011, PhRvL, 106, 174502
Aluie, H. 2013, PhyD, 247, 54
Beaumont, C. N., Goodman, A. A., Alves, J. F., et al. 2012, MNRAS, 423, 2579
Burgers, J. 1948, Advances in Applied Mechanics, Vol. 1 (Amsterdam: Elsevier), 171
Chen, H. H.-H., Pineda, J. E., Goodman, A. A., et al. 2019a, ApJ, 877, 93
Chen, H. H.-H., Pineda, J. E., Offner, S. S. R., et al. 2019b, ApJ, 886, 119
Colombo, D., Hughes, A., Schinnerer, E., et al. 2014, ApJ, 784, 3
Dame, T. M., Elmegreen, B. G., Cohen, R. S., & Thaddeus, P. 1986, ApJ, 305, 892
Dobbs, C. L., Burkert, A., & Pringle, J. E. 2011, MNRAS, 413, 2935
Donovan Meyer, J., Koda, J., Momose, R., et al. 2013, ApJ, 772, 107
Duarte-Cabral, A., Colombo, D., Urquhart, J. S., et al. 2021, MNRAS, 500, 3027
Eden, D. J., Moore, T. J. T., Currie, M. J., et al. 2020, MNRAS, 498, 5936
Elmegreen, B. G., & Scalo, J. 2004, ARA&A, 42, 211
Fleck, R. C., Jr. 1983, ApJL, 272, L45
Goodman, A. A., Barranco, J. A., Wilner, D. J., & Heyer, M. H. 1998, ApJ, 504, 223
Heyer, M., Krawczyk, C., Duval, J., & Jackson, J. M. 2009, ApJ, 699, 1092
Heyer, M. H., & Brunt, C. M. 2004, ApJL, 615, L45
Heyer, M. H., Carpenter, J. M., & Snell, R. L. 2001, ApJ, 551, 852
Hughes, A., Meidt, S. E., Colombo, D., et al. 2013, ApJ, 779, 46
Iroshnikov, P. S. 1964, SvA, 7, 566
Kolmogorov, A. 1941, DoSSR, 30, 301
Kraichnan, R. H. 1965, PhFl, 8, 1385
Krieger, N., Bolatto, A. D., Koch, E. W., et al. 2020, ApJ, 899, 158
Kritsuk, A. G., Lee, C. T., & Norman, M. L. 2013, MNRAS, 436, 3247
Kritsuk, A. G., Norman, M. L., Padoan, P., & Wagner, R. 2007, ApJ, 665, 416
Larson, R. B. 1981, MNRAS, 194, 809
Mandelbrot, B. B. 1983, The Fractal Geometry of Nature, Revised and Enlarged Edition (New York: W. H. Freeman)
McKee, C. F., & Ostriker, E. C. 2007, ARA&A, 45, 565
Myers, P. C. 1983, ApJ, 270, 105
Narayanan, G., Heyer, M. H., Brunt, C., et al. 2008, ApJS, 177, 341
Ridge, N. A., Di Francesco, J., Kirk, H., et al. 2006, AJ, 131, 2921
Ripple, F., Heyer, M. H., Gutermuth, R., Snell, R. L., & Brunt, C. M. 2013, MNRAS, 431, 1296
Roman-Duval, J., Jackson, J. M., Heyer, M., Rathborne, J., & Simon, R. 2010, ApJ, 723, 492
Sofue, Y. 2017, PASJ, 69, R1
Solomon, P. M., Rivolo, A. R., Barrett, J., & Yahil, A. 1987, ApJ, 319, 730
Stone, J. M., Ostriker, E. C., & Gammie, C. F. 1998, ApJL, 508, L99